Ultrafast Polarization Shaping with Fano Plasmonic Crystals

M. R. Shcherbakov,[1] P. P. Vabishchevich,[1] V. V. Komarova,[1] T. V. Dolgova,[1] V. I. Panov,[1]
V. V. Moshchalkov,[2] and A. A. Fedyanin[1,*]

[1]*Faculty of Physics, Lomonosov Moscow State University, Moscow 119991, Russia*
[2]*INPAC-Institute for Nanoscale Physics and Chemistry, KU Leuven, Celestijnenlaan 200 D, B-3001 Leuven, Belgium*
(Received 28 September 2011; published 20 June 2012)

Femtosecond-scale polarization state shaping is experimentally found in optical response of a plasmonic nanograting by means of time-resolved Stokes polarimetry. Simultaneous measurements of the Stokes parameters as a function of time reveal a remarkable alteration of the polarization state inside a single femtosecond pulse reflected from a plasmonic crystal due to the excitation of time-delayed polarization-sensitive surface plasmons with a highly birefringent Fano-type spectral profile. Time-dependent depolarization, indicating the sub-130-femtosecond polarization change inside the pulse, is experimentally found and described within an analytical model which predicts the fivefold enhancement of the polarization conversion effect with the use of a narrower time gate.

DOI: 10.1103/PhysRevLett.108.253903 PACS numbers: 42.70.−a, 06.60.Jn, 73.20.Mf, 78.67.−n

Polarization is a fundamental property of an electromagnetic wave which describes the time-averaged trajectory of the electric field vector at a given point of space. The time scale over which the polarization is averaged is usually much greater than the period of a single electromagnetic field oscillation. However, various methods of femtosecond polarization shaping were proposed recently [1–6] which stimulated intense research in the field of quantum control [7,8]. While many methods of femtosecond polarization shaping rely on conventional macro-scale optical devices, it is also possible to shape the polarization utilizing elementary excitations in submicron quantum-confined media [9,10]. A convenient and easily tunable system for observing elementary excitations at room temperature is a spatially modulated surface of a noble metal film where surface plasmon polaritons (SPPs) are excited. Proved by numerous experiments involving femtosecond laser pulse sources [11–13], the mean lifetime of a resonantly excited SPP varies from tens to hundreds of femtoseconds in the visible and near IR spectral range peaking for dark modes, e.g., in SPP band gap structures or plasmonic crystals [11,12]. On the other hand, remarkable polarization-sensitive properties of plasmonic nanostructured media [14,15] make it possible to use plasmonic nanostructures as polarizers [16] or wave plates [17,18]. Despite high polarization performance and distinct temporal characteristics of anisotropic plasmonic materials, the ultrafast light polarization control with plasmonic media has not been observed yet.

In this Letter, we use time-delayed optical anisotropy of resonantly excited surface plasmon polaritons to realize an ultrafast control over the state of polarization (SoP) inside a single subpicosecond telecom laser pulse reflected from a plasmonic crystal of subwavelength thickness. Time-dependent nonzero depolarization has been found which indicates the sub-130-femtosecond polarization change inside the pulse. Experimental data are supported by an analytic model that predicts the fivefold enhancement of polarization conversion efficiency which makes plasmonic crystals a promising compact media for ultrafast polarization control at room temperature.

The concept of the ultrafast polarization control with anisotropic plasmonic crystals, schematically depicted in Fig. 1, is based on the time-delayed nature of the SPP response. Incident pulse's SoP is split into two linear eigenmodes due to anisotropy of the sample and the p-polarized component is time delayed via exciting SPPs. As a result, femtosecond polarization alteration is expected in the reflected pulse.

Observation of the ultrafast polarization shaping was performed on samples of plasmonic crystals fabricated by thermal sputtering of a gold film onto a polymer grating

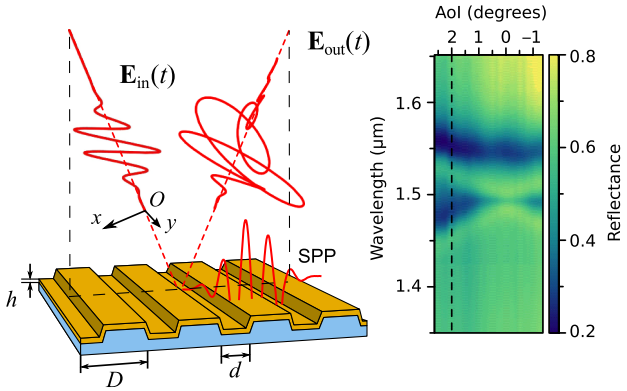

FIG. 1 (color online). Left: schematics of the ultrafast polarization conversion with plasmonic crystals. Sample dimensions are $D = 1.5$ μm, $d = 0.3$ μm and $h = 50$ nm. Right: reflectance of the sample as a function of wavelength and angle of incidence (AoI) for p-polarized incident light. The dashed line denotes the AoI used for the ultrafast polarization conversion.

made by nanoimprint lithography. The following dimensions of the structure were chosen to match the SPP resonances spectral position to the central wavelength $\lambda = 1.56$ μm of the femtosecond laser source: the period is $D = 1.5$ μm, the duty cycle is $d/D = 0.2$ and the film thickness is $h = 50$ nm. The reflection spectra of the sample measured with p-polarized light with its E-vector perpendicular to the grating modulation are shown in Fig. 1. The minima associated with the band structure of SPPs coupled onto the surface of the film via the ± 1st diffraction orders are revealed. The plasmonic band gap is seen at the wavelength $\lambda = 1.52$ μm with the width of $\Delta\lambda \simeq 70$ nm, $\Delta\lambda/\lambda \simeq 0.04$ which is comparable to the previous data on spectroscopy of plasmonic crystals [11,12,19].

Time-resolved response of the plasmonic crystal in s and p-polarized light was studied to determine the plasmonic impact on the femtosecond pulse shape. An Er^{3+}-doped fiber laser (Avesta Project Ltd.) produced a 130 femtosecond pulse train at a telecom central wavelength of $\lambda = 1.56$ μm. The beam was split into two channels one being the gating channel with an optical delay line and another being the signal channel where the sample was illuminated under 2° incidence. The beams were co-focused onto a BBO crystal where the noncollinear second harmonic radiation was generated. Fourth-order correlation functions (CFs) $S(\tau) = \int_{-\infty}^{\infty} |E_{\text{gate}}(\tau - t)|^2 |E(t)|^2 dt$, where $E_{\text{gate}}(t)$ is the field in the gating channel and $E(t)$ is the field in the signal channel, were measured by varying the time delay τ between the pulses. The results of CF measurements for p and s-polarized incident light shown in the inset of Fig. 2 demonstrate a considerable alteration of the femtosecond pulse shape by SPPs. A delay of about 180 fs is seen between the maxima of the CFs measured for orthogonal input SoPs.

Symmetry considerations require s- and p-polarized states to be the eigenstates of the system under study: if the incident pulse is s or p polarized the SoP of the reflected pulse remains constant. However, the evolution of the SoP inside a single pulse becomes complicated if one sends a linear combination of these states onto the plasmonic crystal. Observation of the temporal SoP shaping was done by time-resolved Stokes polarimetry. The schematics of the setup is provided in Fig. 2. The input SoP is prepared by a quarter-wave plate and a Glan-Taylor prism with the latter oriented at an angle ψ with respect to the Oy axis. The pulse reflected from the sample is transformed by a half-wave plate (HWP) and a photoelastic modulator (PEM, Hinds Instruments Inc.) and analyzed by a Glan-Taylor prism. The analyzed pulse contains the temporal evolution of a particular Stokes vector coordinate at different harmonics of the PEM operating frequency. The pulse containing the information about the Stokes vector components is gated by the 130 femtosecond reference pulse and detected by a photomultiplier tube. The signal from the detector is decomposed into f and $2f$

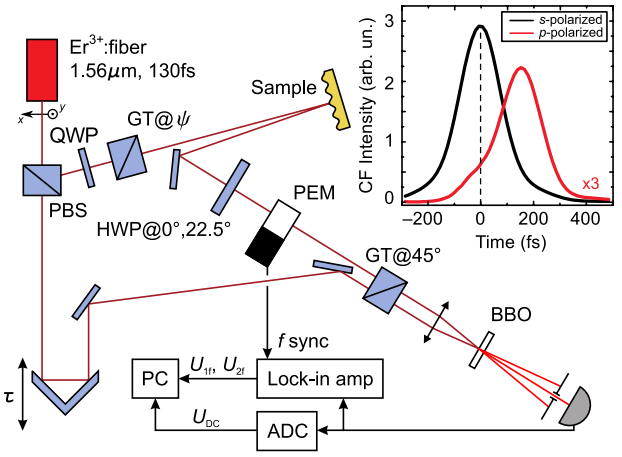

FIG. 2 (color online). Schematics of the time-resolved Stokes polarimetry. Axes Ox and Oy are defined with respect to the wave vector as shown at the laser output. PBS is a polarizing beam splitter, QWP is a quarter-wave plate at 45° with respect to the Oy axis, GT@ψ is a Glan-Taylor polarizer oriented at an angle of ψ with respect to the Oy axis, HWP is a half-wave plate, PEM is a photoelastic modulator, GT@45° is a Glan-Taylor analyzer oriented at an angle of 45° with respect to the Oy axis. The inset shows the correlation functions measured with the U_{DC} signal at $\psi = 0°$ (s polarized, black curve) and $\psi = 90°$ (p polarized, red curve).

harmonics and to dc signal which are proportional to the corresponding Stokes parameters values:

$$\mathbf{S}(\tau) \equiv \begin{pmatrix} S_0(\tau) \\ S_1(\tau) \\ S_2(\tau) \\ S_3(\tau) \end{pmatrix} \sim \begin{pmatrix} U_{\text{DC}} \\ U_{2f}(22.5°) \\ U_{2f}(0°) \\ U_{1f}(22.5°) \end{pmatrix}, \tag{1}$$

where the numbers in brackets denote the angular position of the HWP. This technique allows for the time-resolved measurements of all the Stokes vector components evolution inside the beam reflected from the sample in only two delay line scans performed for 0° and 22.5° of the HWP orientation.

Figure 3 shows the intra-pulse SoP evolution for different ψ values in terms of normalized Stokes parameters $s_i \equiv S_i/S_0$. For $\psi = 0°$ the SoP is a linearly Oy-polarized state for any time moment within the uncertainty of the method which is below 0.1 on the scale of Stokes parameter values. As ψ is increased the modification of the SoP can be seen towards the end of the pulse. Various polarization transformations are observed at femtosecond time scales; e.g., switching between linearly polarized (aspect ratio 0.1) and right-hand circularly polarized (aspect ratio 0.8) is achieved in 100 fs at $\psi = 20°$. Depolarization induced by the sample is seen in time dependences of the degree of polarization defined as $\text{DoP} \equiv \sqrt{s_1^2 + s_2^2 + s_3^2}$ in Fig. 3(e). The depolarization is a consequence of Stokes

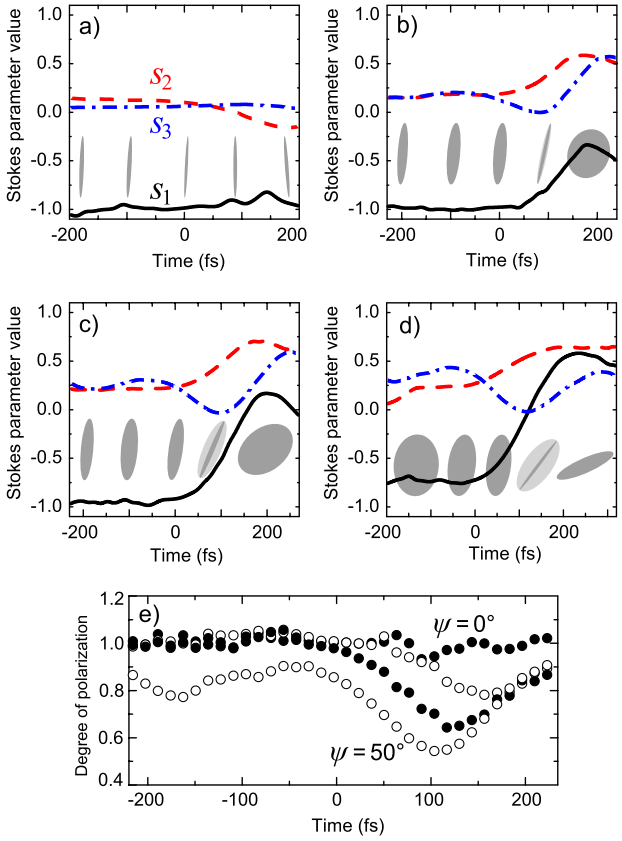

FIG. 3 (color online). (a)–(d) Experimental time-resolved normalized Stokes parameters s_1 (solid lines), s_2 (dashed lines) and s_3 (dotted-dashed lines) of the femtosecond pulse reflected from the plasmonic crystal for different incident SoPs with $\psi = 0°$, 20°, 35°, 50°, respectively. Series of ellipses illustrates the mean trajectory of the E-field vector at $\tau = -200$, -100, 0, 100 and 200 fs, respectively. Gray stands for the coherent component of the SoP and light gray stands for the depolarized one. The sign of s_3 defines the handedness of the SoP—right-handed for positive and left-handed for negative values of s_3. (e) Time-resolved degree of polarization of the reflected pulse SoP for the aforementioned ψ values.

parameters averaging over the 130 femtosecond gate which is discussed below.

The efficiency of the polarization conversion could be described by the polarization conversion rate in the Stokes vector space. It is defined as $v_s = |\mathbf{s}'(t)| = (\sum_{i=1}^{3}(ds_i/dt)^2)^{1/2}$ and represents the speed at which the end of the Stokes vector is moving in the Stokes vector space. The experimental map of v_s is displayed in Fig. 4(a) as a function of τ and ψ. The maximal v_s value is experimentally found to be 14 ps^{-1} which is more than twice the maximal rate achieved in much thicker samples of Bragg-spaced quantum wells at 80 K [9].

The ultrafast polarization conversion is closely related to the optical anisotropy of the plasmonic crystal, which was characterized in CW using the spectrally-resolved ellipsometry setup based on a PEM [20]. The ellipsometric

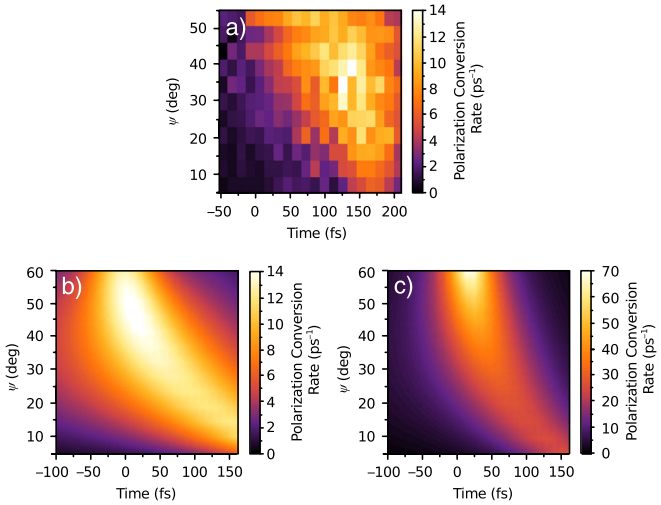

FIG. 4 (color online). (a) Experimental polarization conversion rate as a function of τ and ψ. The maximal value of the rate is equal to 14 ps^{-1} at $\psi = 35°$ and $\tau = 125$ fs. (b), (c) Polarization conversion rate calculated with the gates of 130 and 10 fs, respectively.

parameters $\rho(\lambda)$ and $\varphi(\lambda)$ of the sample define the Jones matrix in the basis of horizontally, (1,0), and vertically, (0,1), polarized waves given as:

$$J(\lambda) \propto \begin{pmatrix} \rho(\lambda)\exp[\imath\varphi(\lambda)] & 0 \\ 0 & 1 \end{pmatrix}. \quad (2)$$

Here, $\rho(\lambda)$ stands for the ratio between the field reflection coefficients of p-polarized and s-polarized light and represents linear dichroism; $\varphi(\lambda)$ is the phase delay introduced into one of these states and represents linear birefringence. Eq. (2) also applies to an optically anisotropic interface if its optical axis is oriented parallel or perpendicular to the plane of incidence. The spectra $\rho(\lambda)$ and $\varphi(\lambda)$ of the sample for 2° incidence are given in Fig. 5. The dichroism spectrum $\rho(\lambda)$ has two minima corresponding to the reflection minima at the plasmonic band gap edges. The phase delay spectrum $\varphi(\lambda)$ experiences a jump from 0 to 1.8π at the long wavelength edge of the band gap. The vast phase jump could be understood in terms of the Fano-type response of the grating [21] resulting from the interference of the specularly reflected light and light coherently reradiated by the SPP scattering. The long wavelength parts of the curves are fitted by the following expressions:

$$T(\omega) = C + \frac{Be^{i\phi}}{\omega - \omega_0 - i\gamma}; \quad (3)$$

$$\varphi(\omega) = \arg T(\omega) - \varphi_0; \qquad \rho(\omega) = |T(\omega)|. \quad (4)$$

The best fit to the experimental data with the parameters of $C = 1$, $B = 2 \times 10^{13}$ rad/s, $\phi = 1.57$ rad, $\omega_0 = 1.205 \times 10^{15}$ rad/s ($\lambda_0 = 1563$ nm), $\gamma = 1.34 \times 10^{13}$ rad/s ($\Delta\lambda = 15$ nm) and $\varphi_0 = 0.2$ rad is shown in

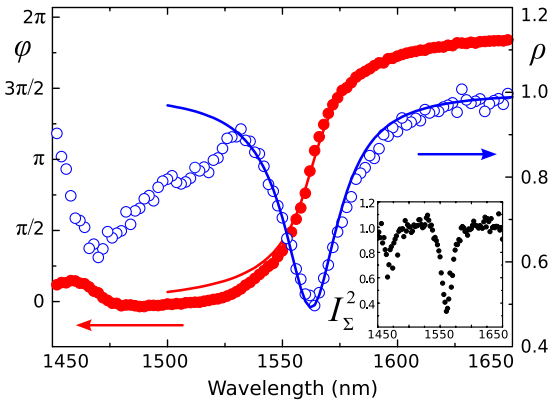

FIG. 5 (color online). Spectra of linear birefringence $\varphi(\lambda)$ (filled dots) and dichroism $\rho(\lambda)$ (empty dots) of the plasmonic crystal at the plasmonic band gap edges. The solid curves denote the best fit of the experimental data to the Eqs. (3) and (4). The inset shows the spectrum of I_Σ^2 which is a measure of depolarization caused by the sample.

Fig. 5 by solid lines. The spectral position of the resonance overlaps with the spectral span of the femtosecond pulses. Each spectral component of an incident femtosecond pulse gains its own phase difference between the s- and p-polarized waves that explains the complicated temporal pulse polarization structure.

In order to determine unambiguously the values of ρ and φ three quantities were measured independently, namely, $I_1 = (\rho^2 - 1)/(\rho^2 + 1)$, $I_2 = 2\rho\sin\varphi/(\rho^2 + 1)$, and $I_3 = 2\rho\cos\varphi/(\rho^2 + 1)$. In a system described by Eq. (2) the condition $I_\Sigma^2 = I_1^2 + I_2^2 + I_3^2 = 1$ holds; the experimental deviation of I_Σ^2 from unity indicates the depolarization the system brings into the beam. The experimental spectrum of I_Σ^2 is plotted as a function of the wavelength in the inset of Fig. 5. Light depolarization with the plasmonic crystal is seen at the edges of the band gap. It is attributed to the spread of the incident beam tangential wave vector component Δk. The latter becomes significant when $\Delta k l > 1$ [22], where l is the SPP mean free path. The divergence of the incident beam in CW measurements was 0.04 that makes $\Delta k l \simeq 1.2$ giving the grounds for the depolarization of light with the sample. Contrary to this, the divergence of the femtosecond laser beam is much smaller resulting in $\Delta k l \simeq 10^{-2}$. It means that the observed time-dependent depolarization is not caused by the spatial inhomogeneity of the incident beam.

The depolarization induced by the sample in the ultrafast experiments is of different nature and can be eliminated by the use of a narrower time gate. The depolarization appears due to averaging of the measured Stokes parameters values within the 130 femtosecond gate and nonunity DoP value observed in Fig. 3(e) means that the polarization conversion happens faster than the gate span. To prove this we apply a model of optical response dynamics based on the spectral response of the plasmonic crystal. If a p-polarized pulse with the Gaussian temporal profile:

$$E_{\text{in}}^p(t) = E_0 e^{-t^2/2\sigma^2} e^{i\omega_0 t}, \tag{5}$$

is incident on the surface of the plasmonic crystal its shape undergoes changes as evidenced by the inset of Fig. 2. The resulting pulse shape originates from the convolution theorem and its explicit form is as follows:

$$E_{\text{out}}^p(t) = \frac{1}{\sqrt{2\pi}} \int_{-\infty}^{\infty} E_{\text{in}}(\tau) T(t-\tau) d\tau, \tag{6}$$

where $T(t)$ is the response of the Fano resonance to the delta excitation expressed as:

$$\begin{aligned} T(t) &= \frac{1}{\sqrt{2\pi}} \int_{-\infty}^{\infty} T(\omega) e^{i\omega t} dt \\ &= \sqrt{2\pi}[C\delta(t) + iB\Theta(t) e^{i\phi + i\omega_0 t - \gamma t}], \end{aligned} \tag{7}$$

where $\Theta(t)$ is Heaviside step function. The explicit expression for the shape of the p-polarized reflected pulse is:

$$\begin{aligned} E_{\text{out}}^p(t) = {} & C E_0 e^{-t^2/2\sigma^2} e^{i\omega_0 t} \\ & + i\sqrt{\frac{\pi}{2}} \sigma B E_0 e^{\sigma^2\gamma^2/2} e^{i\phi + i\omega_0 t - \gamma t} \\ & \times \left[1 + \operatorname{erf}\left(\frac{t - \gamma\sigma^2}{\sigma\sqrt{2}}\right)\right], \end{aligned} \tag{8}$$

where $\operatorname{erf}(x)$ is the error function. In the experiment, the input polarization state is composed out of two linear modes: $\mathbf{E}_{\text{in}} = \mathbf{x}E_{\text{in}}^p + \mathbf{y}E_{\text{in}}^s$, where $E_{\text{in}}^p/E_{\text{in}}^s = \tan\psi$. Describing s-polarized reflected component with an unperturbed Gaussian pulse $E_{\text{out}}^s(t) = E_{\text{in}}^s(t)$ one obtains the explicit expression for the dynamics of the output electric field: $\mathbf{E}_{\text{out}} = \mathbf{x}E_{\text{out}}^p + \mathbf{y}E_{\text{in}}^p \cot\psi$, where Eqs. (5) and (8) apply. Using this expression one can directly calculate the dynamics of the Stokes parameters:

$$\begin{aligned} S_0(\tau) &= \overline{E_{\text{out}}^{p*} E_{\text{out}}^p} + \overline{E_{\text{out}}^{s*} E_{\text{out}}^s}, \\ S_1(\tau) &= \overline{E_{\text{out}}^{p*} E_{\text{out}}^p} - \overline{E_{\text{out}}^{s*} E_{\text{out}}^s}, \\ S_2(\tau) &= 2\text{Re}(\overline{E_{\text{out}}^{s*} E_{\text{out}}^p}), \qquad S_3(\tau) = 2\text{Im}(\overline{E_{\text{out}}^{s*} E_{\text{out}}^p}), \end{aligned}$$

where the averaging is taken within the gating pulse: $\bar{x}(\tau) \equiv \int_{-\infty}^{\infty} x(t)|E_{\text{gate}}(\tau - t)|^2 dt$. The modeling of the Stokes parameters dynamics gives satisfactory results in comparison to the experimental data [23]. After calculation of the Stokes parameters the polarization conversion rate $\upsilon_s(\tau, \psi)$ was calculated for two gate width values of 130 and 10 fs. The calculations predict the fivefold enhancement of the maximal polarization conversion rate from 14 to 70 ps^{-1} with the gate narrowing that is shown in Figs. 4(b) and 4(c). The depolarization vanishes down to values of $1 - \text{DoP} = 10^{-4}$ with the use of the 10 femtosecond gate for all time moments which means that experimentally observed time-dependent depolarization is a

consequence of the SoP averaging. Finally, by varying the symmetry of the plasmonic nanostructure and number of plasmonic resonances [24] it should be possible to tailor the polarization shaping performance on demand.

To conclude, ultrafast polarization shaping is observed in plasmonic crystals by means of the time-resolved Stokes polarimetry. An experimental evidence is provided that effective time separation of the polarization states could be done by means of a subwavelength-thickness material. Plasmon-induced birefringence and dichroism with Fano-type spectral shape cause a pronounced shaping of the polarization state inside a single femtosecond telecom laser pulse at the maximal rate of 14 ps^{-1} in the Stokes vector space. The shaping rate it limited by the gating pulse width that is proved by a simple analytical model which predicts the fivefold conversion rate enhancement. The studied plasmonic nanostructure is a subwavelength-thickness device operating at room temperature which can be used for ultrafast polarization control in novel plasmonic circuits and telecommunication devices.

Authors acknowledge assistance of M. F. Al-Shedivat and financial support from Russian Foundation of Basic Research and Ministry of Education and Science of Russia.

*fedyanin@nanolab.phys.msu.ru

[1] T. Brixner and G. Gerber, Opt. Lett. **26**, 557 (2001).
[2] T. Brixner, G. Krampert, P. Niklaus, and G. Gerber, Appl. Phys. B **74**, s133 (2002).
[3] T. Brixner, W. Pfeiffer, and F. J. G. de Abajo, Opt. Lett. **29**, 2187 (2004).
[4] P. Nuernberger, R. Selle, F. Langhojer, F. Dimler, S. Fechner, G. Gerber, and T. Brixner, J. Opt. A: Pure Appl. Opt. **11**, 085202 (2009).
[5] M. Plewicki, S. M. Weber, F. Weise, and A. Lindinger, Appl. Phys. B **86**, 259 (2006).
[6] L. Polachek, D. Oron, and Y. Silberberg, Opt. Lett. **31**, 631 (2006).
[7] C. Brif, R. Chakrabart, and H. Rabitz, New J. Phys. **12**, 075008 (2010).
[8] D. V. Voronine, D. Abramavicius, and S. Mukamel, J. Chem. Phys. **126**, 044508 (2007).
[9] A. E. Paul, J. A. Bolger, A. L. Smirl, and J. G. Pellegrino, J. Opt. Soc. Am. B **13**, 1016 (1996).
[10] E. J. Gansen and A. L. Smirl, J. Appl. Phys. **95**, 3907 (2004).
[11] C. Ropers, D. J. Park, G. Stibenz, G. Steinmeyer, J. Kim, D. S. Kim, and C. Lienau, Phys. Rev. Lett. **94**, 113901 (2005)
[12] A. S. Vengurlekar, A. V. Gopal, and T. Ishihara, Appl. Phys. Lett. **89**, 181927 (2006).
[13] P. P. Vabishchevich, V. O. Bessonov, F. Y. Sychev, M. R. Shcherbakov, T. V. Dolgova, and A. A. Fedyanin, JETP Lett. **92**, 575 (2011).
[14] G. P. Bryan-Brown, J. R. Sambles, and M. C. Hutley, J. Mod. Opt. **37**, 1227 (1990).
[15] R. Gordon, A. G. Brolo, A. McKinnon, A. Rajora, B. Leathem, and K. L. Kavanagh, Phys. Rev. Lett. **92**, 037401 (2004).
[16] N. Yu, Q. J. Wang, C. Pflugl, L. Diehl, F. Capasso, T. Edamura, S. Furuta, M. Yamanishi, and H. Kan, Appl. Phys. Lett. **94**, 151101 (2009).
[17] A. Drezet, C. Genet, and T. W. Ebbesen, Phys. Rev. Lett. **101**, 043902 (2008).
[18] M. R. Shcherbakov, M. I. Dobynde, T. V. Dolgova, D. P. Tsai, and A. A. Fedyanin, Phys. Rev. B. **82**, 193402 (2010).
[19] S. C. Kitson, W. L. Barnes, and J. R. Sambles, Phys. Rev. Lett. **77**, 2670 (1996)
[20] S. N. Jasperson and S. E. Schnatterly, Rev. Sci. Instrum. **40**, 761 (1969).
[21] U. Fano, Ann. Phys. **424**, 393 (1938).
[22] E. Altewischer, C. Genet, M. P. van Exter, J. P. Woerdman, P. F. A. Alkemade, A. van Zuuk, and E. W. J. M. van der Drift, Opt. Lett. **30**, 90 (2005).
[23] See Supplemental Material at http://link.aps.org/supplemental/10.1103/PhysRevLett.108.253903 for the results of Stokes parameters dynamics calculations.
[24] R. U. Tok and K. Şendur, Phys. Rev. A **84**, 033847 (2011).